Lawrence Berkeley Laboratory
UNIVERSITY OF CALIFORNIA

FORMULATION OF THE COULOMB EFFECTS OF SPECTATOR
FRAGMENTS ON PIONS FROM HEAVY ION COLLISIONS

Hafez M.A. Radi, J.O. Rasmussen, J.P. Sullivan,
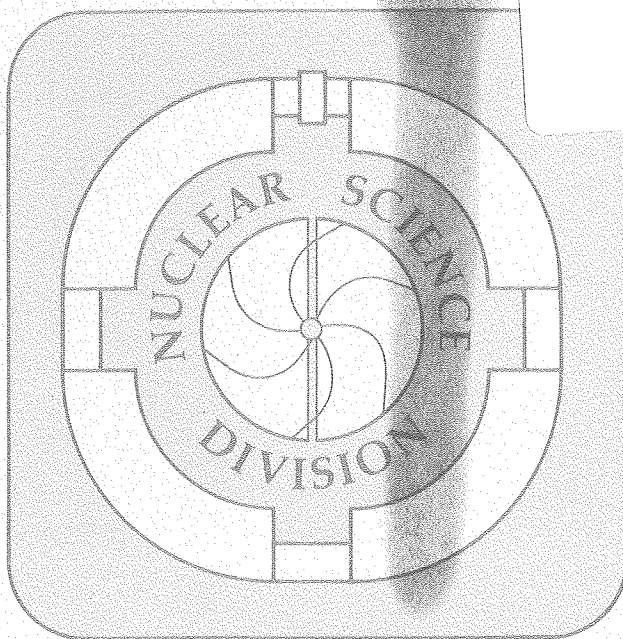K.A. Frankel, and O. Hashimoto

April 1981

DISCLAIMER

Formulation of the Coulomb Effects of Spectator Fragments on Pions from Heavy Ion Collisions

Hafez M.A. Radi
Nuclear Science Division, Lawrence Berkeley Laboratory
University of California, Berkeley, CA 94720
and
Physics Department, Kuwait University, Kuwait

and

J.O. Rasmussen, J.P. Sullivan, K.A. Frankel, and O. Hashimoto*
Nuclear Science Division, Lawrence Berkeley Laboratory
University of California, Berkeley, CA 94720

Abstract

Coulomb effects on heavy-ion pion production cross sections are formulated in terms of weighted averaging over various projectile fragments. Satisfactory fits to zero-degree pion data are found for Ar + C and Ne + C systems. The fragment distributions of excited compound nuclei, before nucleon evaporation, must be used, and the fragment velocity dispersion parameter needed is smaller than that measured for fragments after nucleon evaporation. Average charge Z_{eff} values are determined and compared with those from an experimental paper. In the heavy-ion energy range of the $0°$ pion studies (300 MeV $\lesssim$ E/A $\lesssim$ 600 MeV), it is inferred that target-projectile factorization for fragmentation cross sections does not hold.

KEYWORD ABSTRACT

*On leave from Institute for Nuclear Study, University of Tokyo, Japan.

Introduction

The strong π^- peak and π^+ depression near beam velocity for heavy-ion-produced pions[1] is qualitatively understood as a Coulomb effect of projectile spectator charges.

The theoretical studies of refs. 2, 3, and 4 all show the above effect. In ref. 3 the Coulomb field after the collision was approximated by spreading part of the proton charge along a line between nuclear centers with the remainder continuing with unaltered velocities in the original Gaussian distributions. In ref. 4 various approximate analytical expressions were derived for thermally expanding charge distributions. In particular, the π^-/π^+ ratio at its peak is very sensitive to the temperature assumed for the spectator source, a temperature of ~4 MeV appearing reasonable for the data of ref. 1.

The collaborators of ref. 1 meanwhile upgraded their zero-degree pion spectrometer with wire chambers to measure double differential cross sections at higher resolution than before. The resulting new data[5] show the π^- peak to be considerably sharper than was inferred from the lower resolution spectrometer.

The new data can be fit within the framework of Gyulassy-Kauffmann theory[4]. However, unrealistically low values of the spectator temperature parameter are required to fit the data.

Since production of bound projectile fragments at near-beam velocity is known to be appreciable, these bound fragments ought to be taken explicitly into account in pion-production Coulomb effects. Fortunately, there are some detailed measurements of the momentum shifts and dispersions of fragments at Bevalac energies[6-8]. The systematics of fragment cross sections have been established from experimental and theoretical work of many groups[9-13].

Formulation of Projectile Fragment Coulomb Correction

The Coulomb correction to the pion production cross section depends on the regular Coulomb function $F_\ell(\eta_\pm, \rho_{s_\pm})$[14], where η is the Sommerfeld parameter, $\eta_\pm = \pm\frac{Ze^2}{\hbar v}$, $\vec{v}$ is the velocity of the produced pion relative to the spectator, and Z is the charge of the spectator. For the cases of interest, the s-wave term is predominant in the expansion, and it is a good approximation to write the cross section as[14]

$$\sigma_{\pi\pm} \propto \left| \frac{F_0(\eta_\pm, \rho_{s_\pm})}{\rho_{s_\pm}} \right|^2 \simeq G_\pm (1 + \rho_{s_\pm}\eta_\pm + \ldots)^2 \tag{1}$$

where

$$\rho_{s_\pm} = k_\pm r_s = r_0 \frac{m_\pi c}{\hbar} \beta_{\pi\pm} A_F^{1/3} \qquad \text{with } r_s = r_0 A_F^{1/3} \,,$$

$$G_\pm = \frac{2\pi\eta_\pm}{[\exp(2\pi\eta_\pm)-1]} \,, \tag{2}$$

and the $+,-$ signs stand for π^+ and π^-, respectively.

For comparison with inclusive pion data we should calculate an average value of Eq. (1) over all products and relative velocity of pion and fragment rather than for one set of A, Z, v. The velocity dispersion formula obtained by Greiner et al.[6] is used, and it has the form

$$P \propto \exp\left(-\frac{\beta_F^2}{2\alpha_F^2}\right) \,, \tag{3}$$

where $\beta_F = v_F/c$ is the fragment velocity in units of c, and the velocity dispersion width α_F is given as

$$\alpha_F = \sigma_0 c/(m_N c^2) \sqrt{(A_0 - A_F)/[A_F(A_0-1)]} \,. \tag{4}$$

In eq. (4) the constant σ_0 has been found to be about 86 MeV/c by experiment, $m_N c^2$ is the nucleon rest mass energy constant, A_0 is the projectile mass, and A_F is the mass of fragment under consideration.

Furthermore, the averaging technique requires weighting with respect to the cross section of forming a fragment of mass A_F and charge Z_F, $\sigma(A_F, Z_F)$ before evaporation of protons and neutrons, and also with respect to the differential cross section (before Coulomb correction) of forming a pion simultaneously with a fragment of mass A_F near beam velocity, which is assumed to be a function of the mass loss, $F(A_0 - A_F)$. $\sigma(A_F, Z_F)$ is calculated by the computer code of P. McGaughey and D. Morrissey[15].

It is now straightforward to integrate over β_F and have the analytical formula for the average value of $n_\pm$ in terms of an error function as

$$\langle n_\pm \rangle_{\beta_F} = \pm \left(\frac{Z_F e^2}{\hbar c} \right) \frac{\text{erf}[\beta_{\pi\pm}/(\sqrt{2}\, \alpha_F)]}{\beta_{\pi\pm}} \quad . \tag{5}$$

It is a good approximation to replace the average over β_F in the pion cross section by the average over the Sommerfeld parameter and get the grand average of the pion cross section as

$$\langle \sigma_{\pi\pm} \rangle = \frac{\displaystyle\sum_{A_F, Z_F} N_{A_F} \sigma(A_F, Z_F) F(A_0 - A_F) G_\pm(\langle n \rangle_{\beta_F}) \left\{ 1 + \frac{m_\pi r_0 c}{\hbar} \beta_{\pi\pm} \langle n_\pm \rangle_{\beta_F} A_F^{1/3} \right\}^2}{\displaystyle\sum_{A_F, Z_F} N_{A_F} \sigma(A_F, Z_F) F(A_0 - A_F)} \tag{6}$$

where $N_{A_F} = \sqrt{2\pi}\, \alpha_F^3$.

Numerical Calculations

To employ our code for averaging pion Coulomb effects over projectile fragments, we must have cross sections for fragments as input.

The most nearly applicable fragmentation data are those of Symons et al.[8] on the ^{40}Ar + ^{12}C system, though their measurements were at a different energy, 213 MeV/N, from our pion work at 533 MeV/N.

The data of Lindstrom et al.[9] give ^{16}O and ^{12}C fragmentation at higher energies (and 2 GeV/N). From their data they showed that target factorization holds, that is, that cross sections were expressible as a product of two factors, γ_B^F depending on projectile and fragment N and Z and a target factor γ_T, depending on target mass number. It is evident that the results of fragment averaging by eq. (6) would give a target independence if target factorization held. Such target independence is contrary to the findings of Sullivan et al.[5]

Thus, we sought some theoretical code for fragmentation cross sections. The two main approaches are (1) microscopic Monte Carlo cascade-evaporation models and (2) geometrical abrasion-ablation models of the fireball and firestreak variants. We have been fortunate that Patrick McGaughey at Berkeley had refined the early firestreak code of Oliveira et al.[12] and could immediately run fragmentation calculations for our use. Figure 1 shows a comparison of fragment element yields between the firestreak code and the data of ref. 8. The solid histogram shows the primary yields of excited compound nuclei after the fast stage (abrasion) but before particle evaporation (ablation). The dashed histogram shows the final yields. The comparison with the data is reasonable.

Since the pions should move out many nuclear diameters during a mean life of compound nuclei, it seems more correct to use the primary fragment distribution rather than the final distribution for our pion Coulomb code[14]. Figure 2 shows the results of our theoretical code compared to ^{40}Ar + C experimental pion data of Sullivan et al.[5] The firestreak code fragment yields at 533 MeV/N, slightly broader than those of Fig. 1, were used as input. Here we made the simplest assumption for the pion production factor, namely, purely linear dependence on fragment mass loss $(A - A_F)$. A momentum dispersion constant of $\sigma_0 = 60$ MeV/c and a radius constant $r_0 = 1.5$ fm were used in eq. (6). The theoretical curve was corrected by folding in the experimental resolution. The agreement seems quite satisfactory. In ref. 5 this Ar + C case could not be fit well using Coulomb factors for a single effective Z_F fragment charge. Since the momentum dispersion of primary fragments before particle evaporation is unknown, we did not constrain the calculations to the experimental constant $\sigma_0 = 86$ MeV/c but tried different values.

In Fig. 3 we show McGaughey's firestreak code yields for ^{20}Ne fragmentation at E/A = 280 MeV on a carbon target. In Fig. 4 we show the theoretical cross-section curves compared to data from ref. 5. Both the theory before folding with experimental resolution (dashed) and after folding (solid) are plotted. As in the Ar + C case of Fig. 2 the dispersion width constant σ_0 of 60 MeV/c and r_0 of 1.5 fm were used. It was necessary not only to use the fragment yields before evaporation (Fig. 3 solid curve) but also to further bias the pion production toward heavier fragments by a quadratic term in the pion production factor F, namely,

$$F = N_\pi \left[(A_0 - A_F) + C_\pi (A_0 - A_F)^2 \right],$$

with $C_\pi = -0.06$ and $N_\pi = 0.216$ b.sr^{-1} Gev^{-2}.

It may seem inconsistent that a different F function form was used for neon than for argon. However, if we go back to the Ar + C case and use the quadratic F function for Ne, the comparison with data after folding in experimental resolution is scarcely changed. The theory before resolution shows a higher, sharper π^- peak with the quadratic term, but the experimental resolution is such that the argon data are insensitive to the quadratic coefficient, while the neon data do require such a term.

We have used a smaller production dispersion constant σ_0 than that given by inclusive fragmentation measurements of Greiner et al.[6] and Van Bibber et al.[7] The data really are sensitive to the choice of σ_0, as Fig. 5 makes clear. In Fig. 5 are plotted the data in comparison with theory for three different dispersion constants, σ_0 of 60, 86, and 110 MeV/c. All other parameters are held the same and are the same also as for Fig. 4. For simplicity, the theory before experimental resolution folding is not shown in Fig. 5. It is evident that the smallest value of σ_0 gives the best fit.

In the data fitting of the experimental paper of Sullivan et al.[5], it may seem at first strange that a different effective fragment charge Z_{eff} must be used for π^- and for π^+ data in the same system. Thus, it is gratifying that the detailed fragment averaging of the present paper gives agreement for π^- and π^+ data using all the same parameters (σ_0, C_π, and normalization). Figure 6 shows the theory and data for π^+ in the Ne + C system at E/A = 280 MeV. The same parameters were used as for the π^- case of Fig. 4.

While the formulations of the present paper go beyond those of ref. 5 in doing detailed averaging over projectile fragments (equivalently, impact parameter), they are less complete in another sense in that no account is taken of Coulomb effects of target charge or abraded projectile charge, which are treated in ref. 5.

Thus, we have here restricted our data comparisons to their lightest target, carbon. We should like to use insights from the detailed fragment averaging to interpret qualitatively the significance of pion data on other target systems and at other beam energies. To do this we need to make a connection to the Z_{eff} values determined by Sullivan et al.[5] For our theoretical results of Figs. 2, 4 and 6 we have calculated what single value of average Z_{eff} would give the same Coulomb correction factor for various pion momenta. The results are plotted in Fig. 7. That the values are not constant with momentum is a consequence of the different shapes resulting from detailed averaging over fragments compared to that of a single "average" fragment. We then do a weighted average $\left(\bar{Z}_{eff} = \int_0^{P_{max}} Z_{eff} \; p \; dp / \int_0^{P_{max}} p \; dp \right)$ over the curves of Fig. 6. The results are given in Table I and compared to those of Sullivan et al.[5] Let us now examine and interpret the trends in Z_{eff-}, as they are better determined than Z_{eff+}. From Fig. 20 of ref. 5 we see that Z_{eff-} increases monotonically with target mass through the sequence Ne + C, NaF, Cu, and U. Such a target dependence of Z_{eff-} rules out target factorization, as mentioned earlier. The target dependence is a natural consequence of the geometrical nature of the abrasion process; larger target nuclei "scrape out" broader distributions of projectile fragments. The Z_{eff-} values of ref. 5 show a slight decrease with bombarding energy. It is natural to attribute that decrease also to a broadening fragment distribution.

The firestreak abrasion code of McGaughey that was used in the present work evidently reproduces target mass dependence reasonably well but has too little dependence of abrasion product distribution on bombarding energy.

It is satisfying to see that pion spectral features are quantitatively explained in terms of Coulomb effects of abrasion fragments before evaporation of additional charge. The need for the somewhat smaller momentum dispersion constant σ_0 than that of inclusive fragmentation experiments is an interesting feature, suggesting smaller velocity dispersion of primary fragments. On the theoretical side this approach needs extension to incorporate anisotropic fragment momentum dispersions. Also it would be desirable to incorporate Coulomb effects of target charge. On the experimental side we look forward to the more detailed information of pion heavy fragment correlation data in future work.

References

1. W. Benenson, G. Bertsch, G.M. Crawley, E. Kashy, J.A. Nolen, Jr., H. Bowman, J.G. Ingersoll, J.O. Rasmussen, J. Sullivan, M. Koike, M. Sasao, J. Peter, and T.E. Ward, Phys. Rev. Lett. 43, 683 (1979).

2. G. Bertsch, Phys. Rev. C15, 713 (1977).

3. K.G. Libbrecht and S.E. Koonin, Phys. Rev. Lett. 43, 1581 (1979).

4. M. Gyulassy and S.K. Kauffmann, LBL-10279 (1980), to be published in Nucl. Phys. A.

5. J. Sullivan, et al., Lawrence Berkeley Laboratory report LBL-11971 (1980), submitted to Phys. Rev. C.

6. D.E. Greiner, P.J. Lindstrom, H.H. Heckman, Bruce Cork, and F.S. Bieser, Phys. Rev. Lett. 35, 152 (1975).

7. K. Van Bibber, D.L. Hendrie, D.K. Scott, H.H. Wieman, L.S. Schroeder, J.V. Geaga, S.A. Chessin, R. Treuhaft, J.Y. Grossiord, J.O. Rasmussen, and C.Y. Wong, Phys. Rev. Lett. 43, 840 (1979).

8. T.J.M. Symons, Y.P. Viyogi, G.D. Westfall, P. Doll, D.E. Greiner, H. Faraggi, P.J. Lindstrom, D.K. Scott, H.J Crawford, and C. McParland, Phys. Rev. Lett. 42, 40 (1979).

9. P.J. Lindstrom, D.E. Greiner, H.H. Heckman, B. Cork, and F.S. Bieser, Lawrence Berkeley Laboratory report LBL-3650 (1975), unpublished.

10. J. Hüfner, K. Schäfer, and B. Schurman, Phys. Rev. C12, 1888 (1975).

11. T. Shibata, H. Ejiri, J. Chiba, S. Nagamiya, K. Nakai, R. Anholt, H. Bowman, J.G. Ingersoll, E.A. Rauscher, and J.O. Rasmussen, Nucl. Phys. A308, 513 (1978).

12. L.F. Oliveira, R. Donangelo, and J.O. Rasmussen, Phys. Rev. C19, 826 (1979).

13. D.J. Morrissey, L.F. Oliveira, J.O. Rasmussen, G.T. Seaborg, Y. Yariv, and Z. Fraenkel, Phys. Rev. Lett. 43, 1139 (1979).

14. J.O. Rasmussen, H.M.A. Radi, J. Sullivan, K. Frankel and O. Hashimoto, LBL-12623, Proceedings of the 5th High Energy Heavy Ion Study.

15. P. McGaughey and D. Morrissey, Lawrence Berkeley Laboratory (1981), private communication.
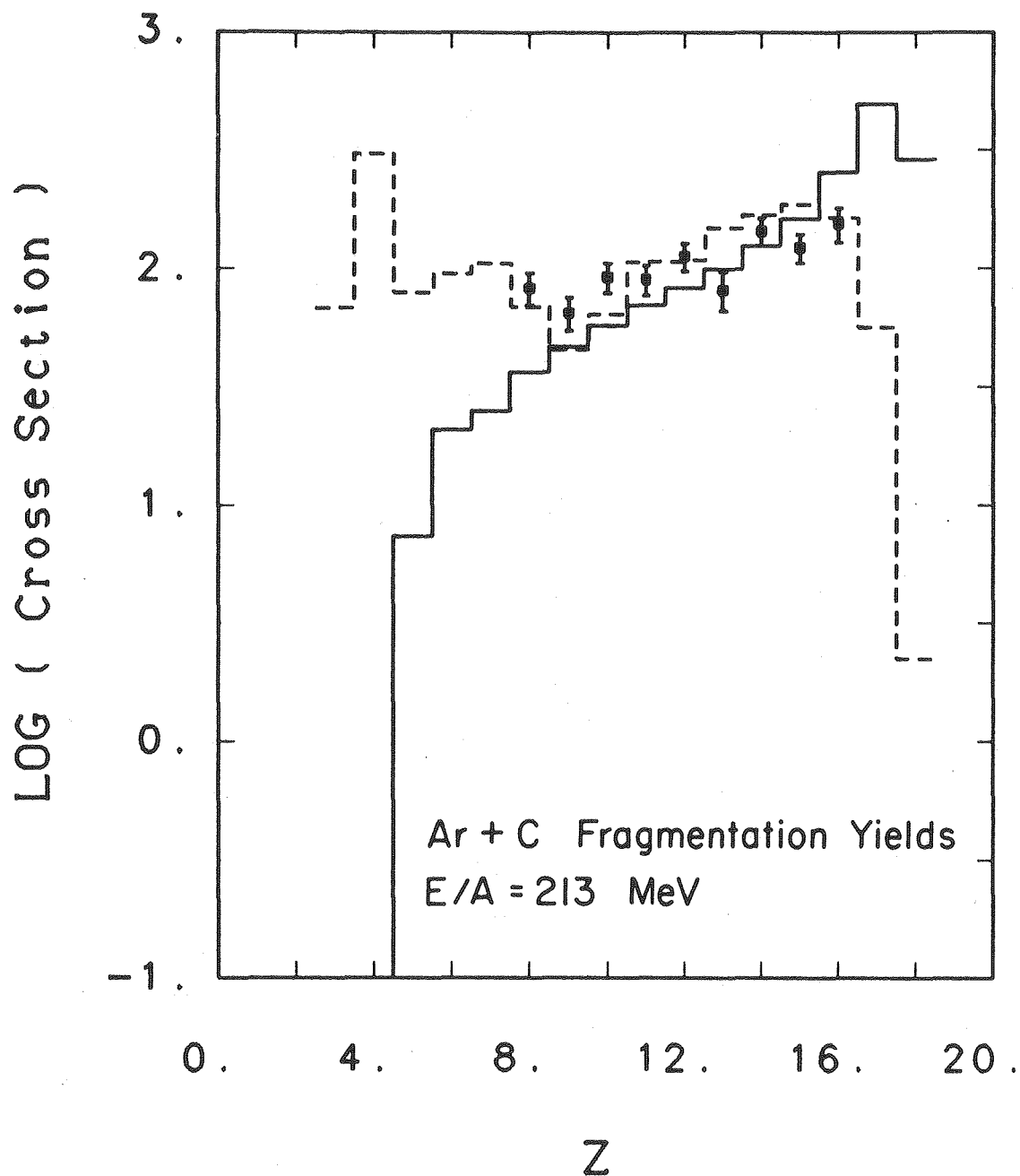
Table I

Comparison of Effective Charge

E_{beam} (MeV/A)	Beam	Target	$\bar{Z}_{eff}$ [a]		Z_{eff} [b]	
			π^-	π^+	π^-	π^+
280	^{20}Ne	^{12}C	4.3	2.9	6.4	3.8
482	^{20}Ne	^{12}C	4.2	2.8	5.0	3.5
533	^{40}Ar	^{12}C	6.1	4.0	6.3	8.4

a) This work

b) Sullivan et al.

Figure Captions

Fig. 1.   Comparison of ^{40}Ar fragment yields for given Z between theory

and experiment. Data points are from Symons et al.[8] at E/A =

213 MeV on a carbon target. The solid (dashed) histogram is the

theoretical distribution before (after) nucleon evaporation

according to the firestreak code of McGaughey. The summed cross

sections are in millibarns.

Fig. 2.   The π^- spectrum at $0°$ calculated by eq. (6) and compared to

data of Sullivan et al.[5] The solid curve is the theory after

folding with experimental resolution. The abscissa is pion

momentum in the projectile frame.

Fig. 3.   Same as Fig. 1, except for ^{20}Ne + ^{12}C at E/A = 280 MeV.

There are no direct fragmentation data for comparison, but this

figure shows input into eq. (6) for calculations shown in Fig. 4.

Fig. 4.   Same as Fig. 2 except for the ^{20}Ne on ^{12}C system at E/A =

280 MeV. The dotted curve is the theory before folding with

experimental resolution, and the solid curve is the theory after

folding.

Fig. 5.   Same as Fig. 4 except that only the theoretical curves after

folding with experimental resolution are shown, and the curves

are given for three different choices of fragmentation velocity

dispersion parameter σ_0.

Fig. 6.   Same as Fig. 4 except for π^+ instead of π^-.

Fig. 7.   The average effective fragment charge Z_{eff} that would give the

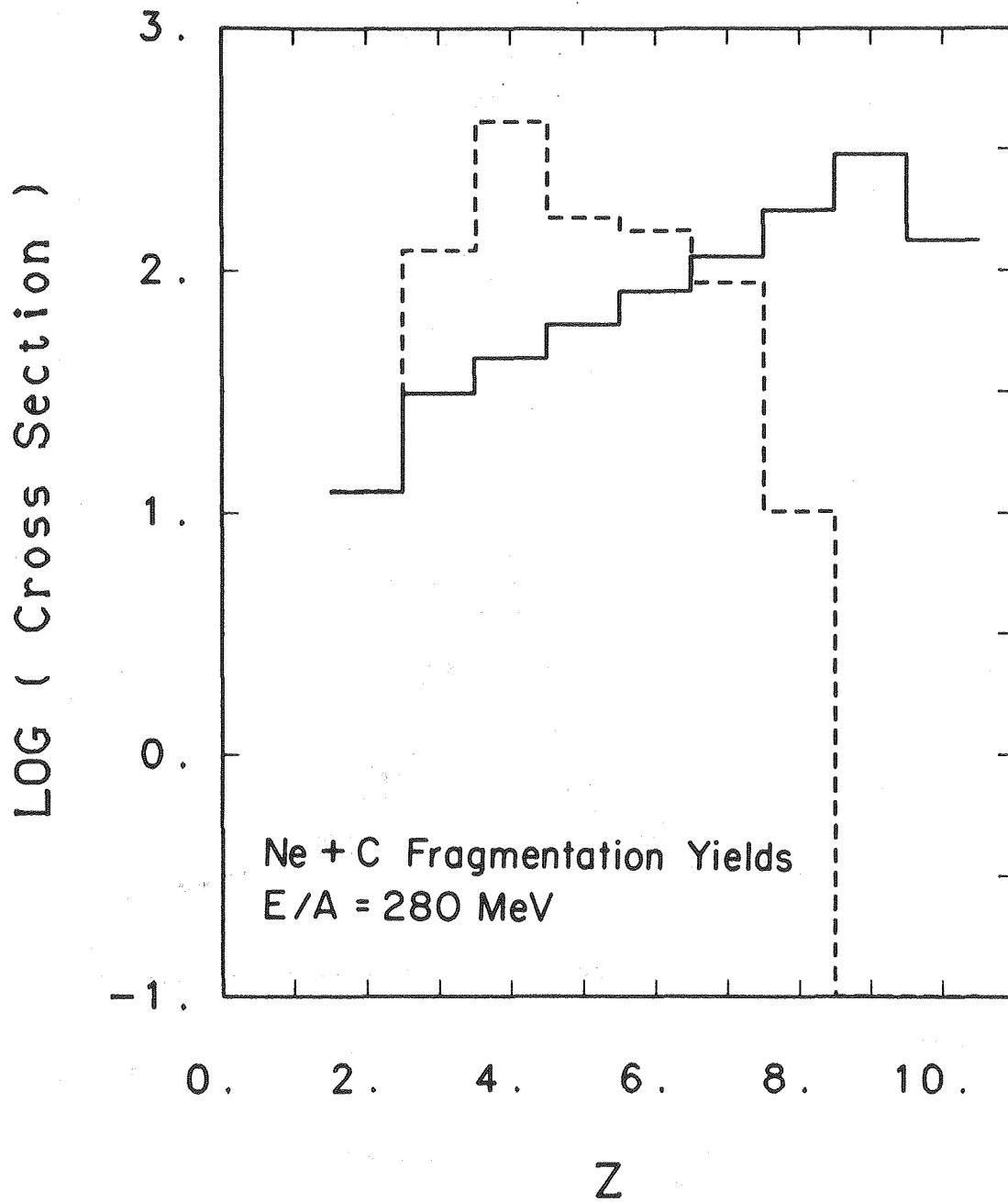same theoretical $\pi^\pm$ cross section as our detailed averaging

eq. (6).

Fig. 1. Comparison of ^{40}Ar fragment yields for given Z between theory and experiment. Data points are from Symons et al.[8] at E/A = 213 MeV on a carbon target. The solid (dashed) histogram is the theoretical distribution before (after) nucleon evaporation according to the firestreak code of McGaughey. The summed cross sections are in millibarns.

Fig. 2.   The π^- spectrum at $0°$ calculated by eq. (6) and compared to data of Sullivan et al.[5] The solid curve is the theory after folding with experimental resolution. The abscissa is pion momentum in the projectile frame.
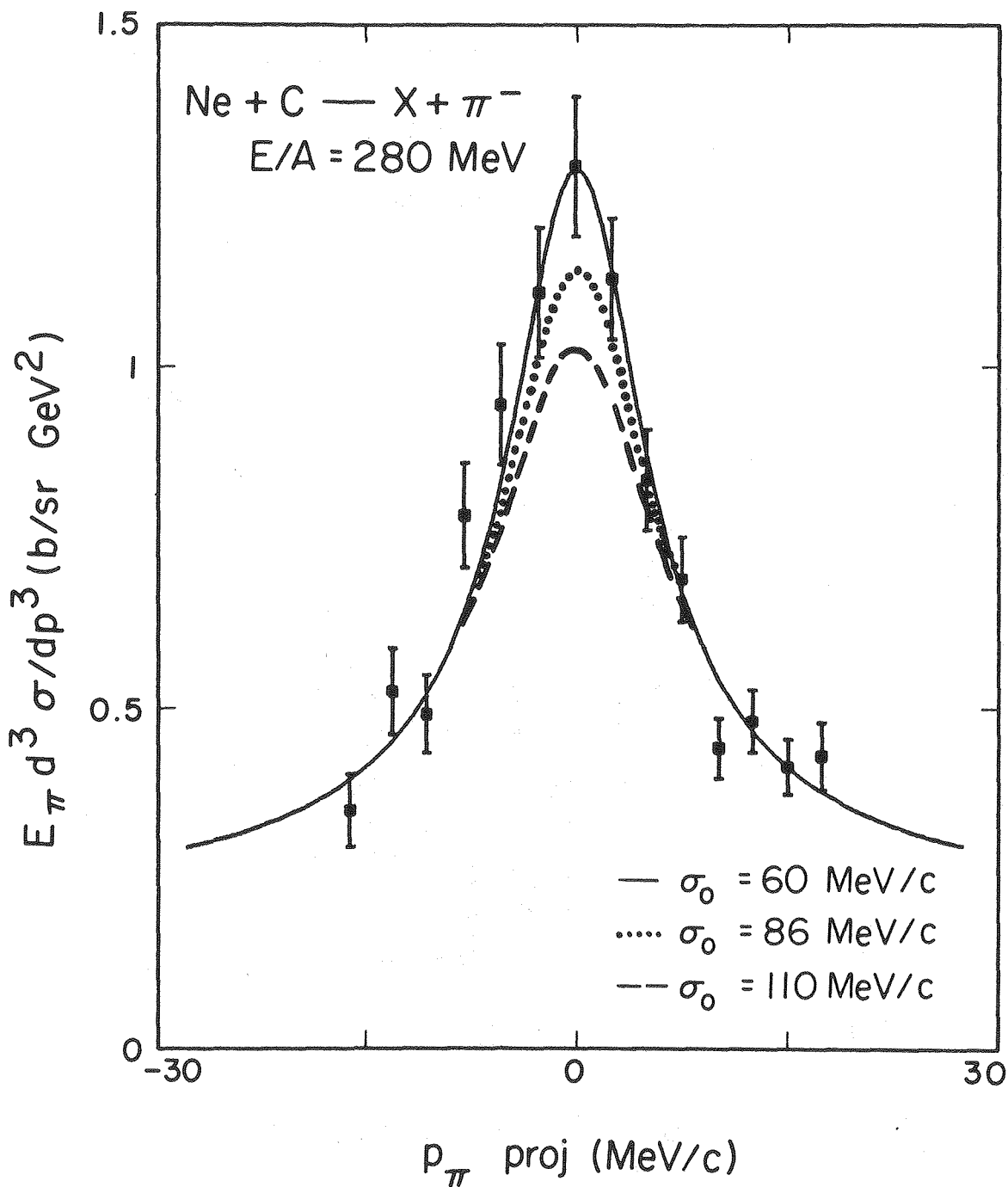
XBL 816-10168

Fig. 3.   Same as Fig. 1, except for ^{20}Ne + ^{12}C at E/A = 280 MeV.

There are no direct fragmentation data for comparison, but this

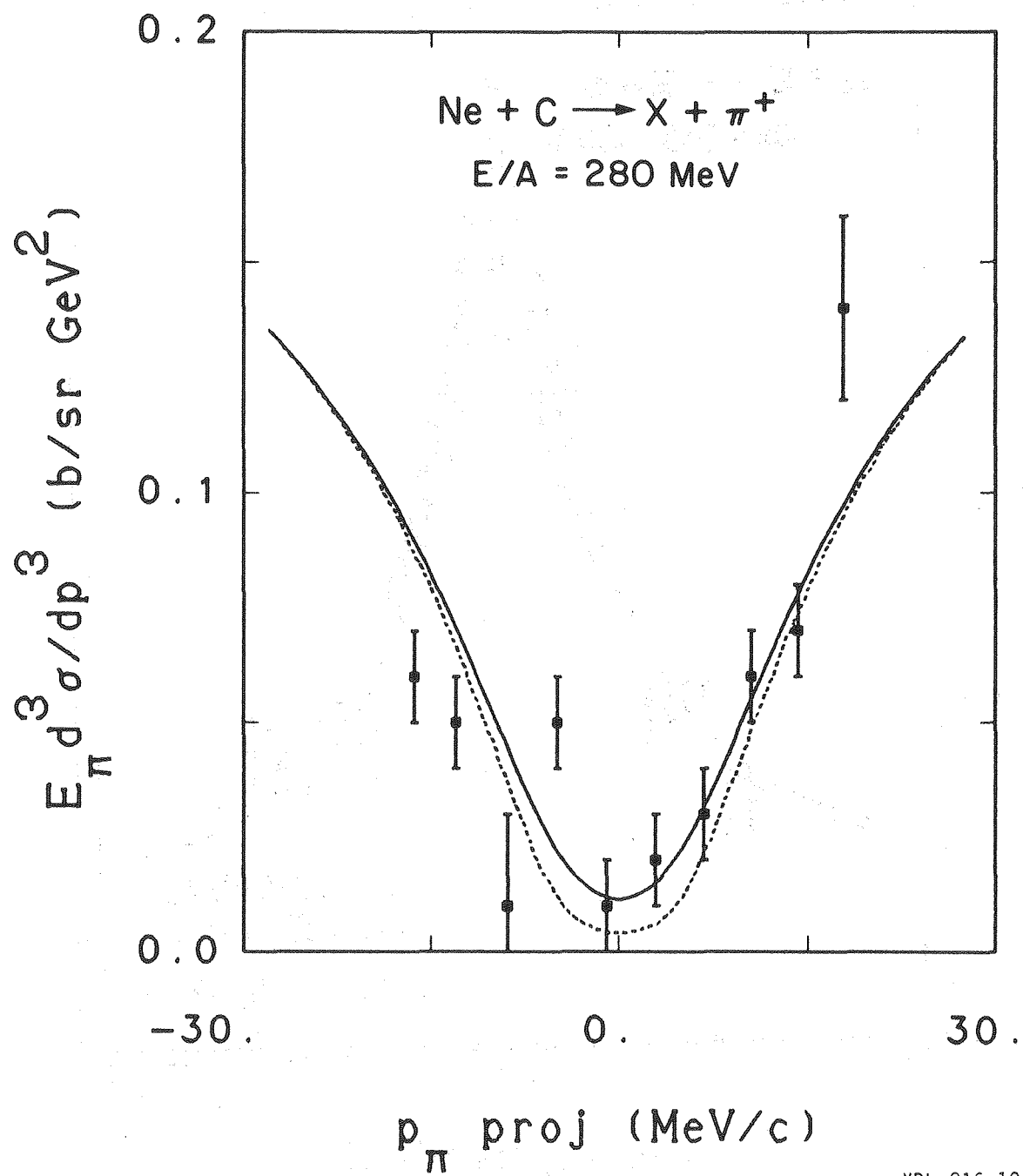figure shows input into eq. (6) for calculations shown in Fig. 4.
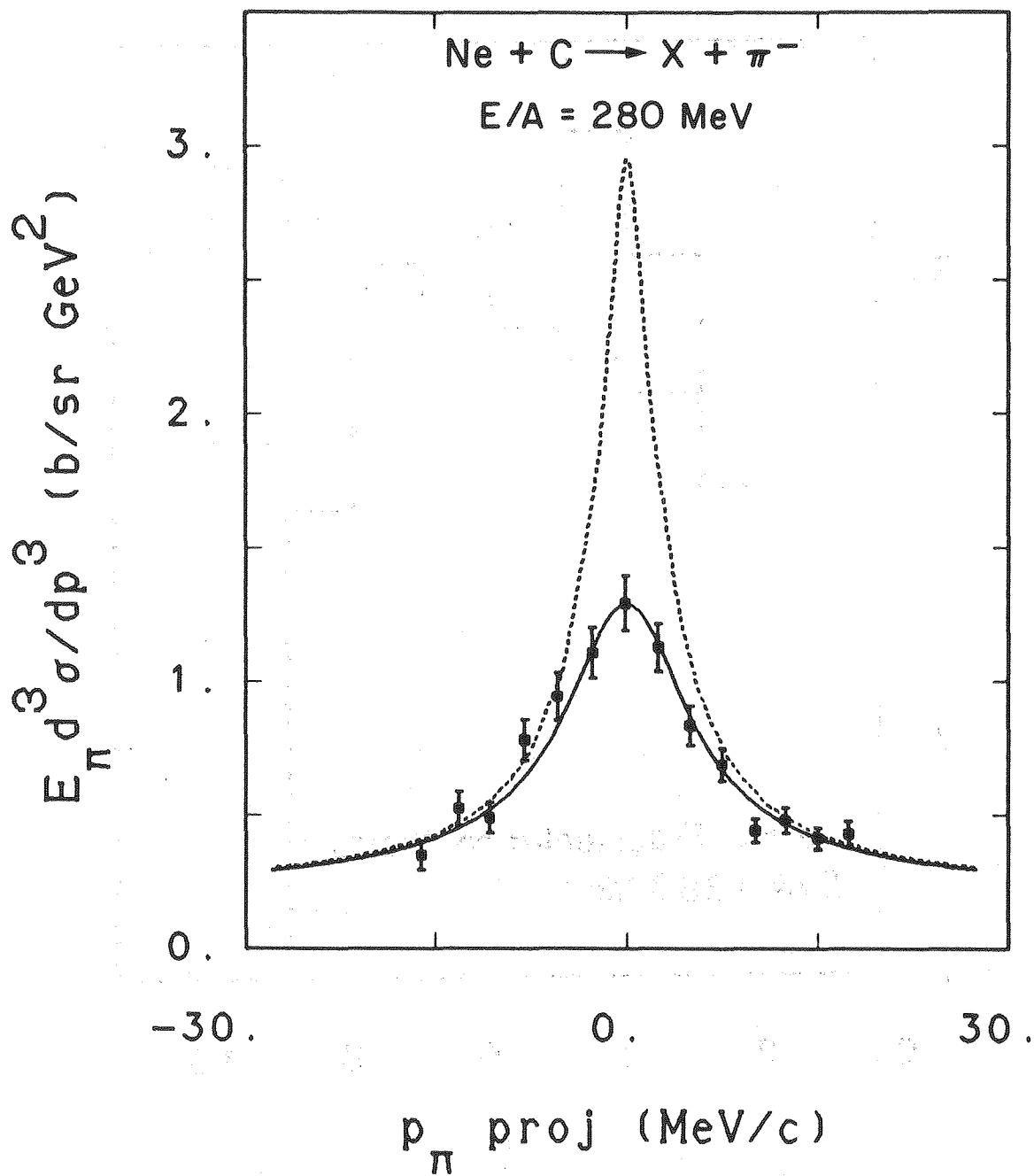
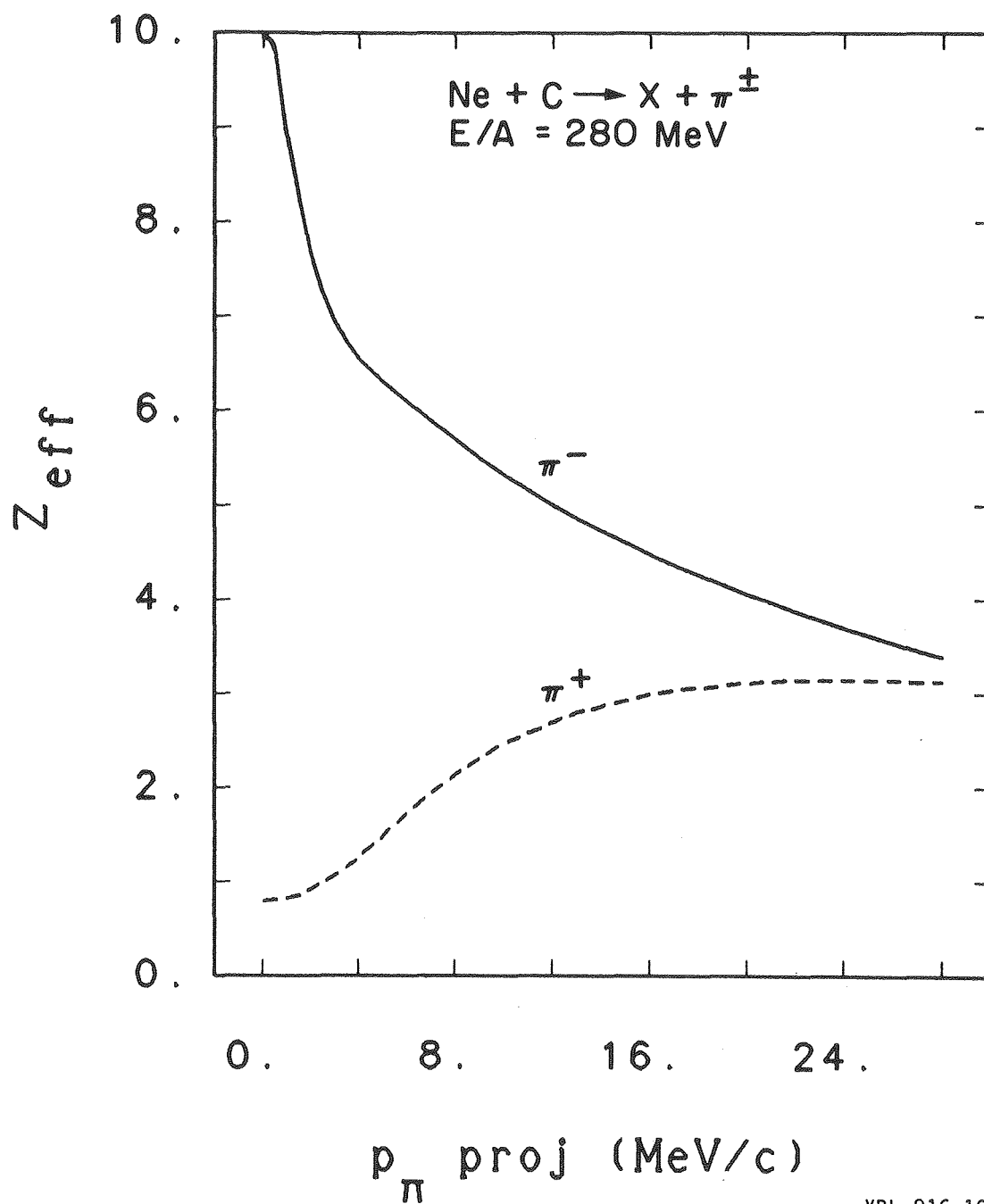Fig. 4. Same as Fig. 2 except for the ^{20}Ne on ^{12}C system at E/A = 280 MeV.

XBL 816-10172

Fig. 5.   Same as Fig. 4 except that only the theoretical curves after folding with experimental resolution are shown, and the curves are given for three different choices of fragmentation velocity dispersion parameter σ_0.

Fig. 6.   Same as Fig. 4 except for π^+ instead of π^-.

Fig. 7. The average effective fragment charge Z_{eff} that would give the same theoretical $\pi^{\pm}$ cross section as our detailed averaging eq. (6).